The Effect of Confinement on Fe_2O_3 Nanoparticles in Free Diffusion and with a Horizontal Magnetic Field

Patrick Simonson, Ashely Rice, Gabrielle Seymore, Ana Oprisan

Department of Physics and Astronomy, College of Charleston

We investigated the magnitude of the confinement effect's influence on the free diffusion of Iron Oxide Fe_2O_3 in pure water contained in cells of different volumes and also that of an applied magnetic field. A shadowgraph apparatus consisting of a super luminous diode (SLD) source, a CCD camera, and achromatic lenses was used to record and analyze the changing indices of refraction due to the presence of concentration-driven fluctuations as the solution diffuses. Extracted frames from this recording were processed through a Differential Dynamic Algorithm (DDA) that determined the dynamics of the process, such as the structure function. The results generated by the DDA was further analyzed to determine how the amplitude of concentration fluctuations change over time and how long those fluctuations are present, revealing a dependency of the dynamics on the size of the cell containing the solution.

Introduction

Fluctuations in free diffusion are caused by the coupling of velocity fluctuations parallel to the driving gradient and the macroscopic concentration gradient [1, 2]. The scale of fluctuations in a concentration gradient is affected by the forces acting on it, namely the gravitational force and the Casimir-like forces exerted by the walls of the cell through a confinement effect [1, 3-5]. This confinement effect is caused by the geometry of a system's cell and affects the strength of the fluctuations. Intensive optical techniques must be utilized to detect the relatively small fluctuations resulting from confinement.

Light scattering techniques can be used to optically investigate the fluctuations' intensities and dynamics. In their work on the shadowgraph technique, Trainoff and Cannell [6] provided the theoretical foundation for experiments carried out using this light scattering method. Briefly, a weak fluctuation in the refractive index diffracts light coherently. The two scattered beams recombine with the transmitted one at the recording plane providing the shadowgraph signal.

Confinement

This technique is useful for investigating the confinement effect as the fluctuations resulting from confinement are weak. Fisher and de Gennes predicted that the confinement of critical fluctuations in a binary liquid mixture gives rise to long-ranged forces between immersed particles. They suggested that these long-ranged forces would eventually lead to the clumping of colloidal particles which are dissolved in a near-critical mixture [7]. The physical origin of this force is similar to the Casimir force between conducting plates, which arises due to the confinement of quantum mechanical vacuum fluctuations of the electromagnetic field [8].

This idea regarding clumping of colloidal particles due to Casimir-like forces requires a generalized approach that could account for fluctuation-enhanced Casimir-like forces in non-equilibrium systems.

Magnetic Nanoparticles

Similarly, spherical magnetic nanoparticles are being extensively tested as a new medicine delivery system by means of an external magnetic field. This process could be used for drug targeting therapy, chemotherapy options, MRI contrast, and immune health [9]. Its advantages include being precise and non-invasive. Magnetic nanoparticles form rod-like structures in the presence of a magnetic field. An applied magnetic field can reduce affect of gravity on the diffusive properties of the system [10].

To understand the nanoparticle solution's potential to be used in this way, the free diffusion process must be thoroughly investigated and compared to data taken with an applied magnetic field. The behavior of the concentration gradient is important to identify along with that of the confinement effect in order to anticipate how these materials would interact in small spaces such as a vein.

We compared the characteristic times of the concentration fluctuations as well as the diffusion coefficients for cell types of varying volumes. The correlation between the volume of the space containing the diffusion process and the time over which diffusion acts on the concentration fluctuations were analyzed. The effect of an applied magnetic field was studied for two of our four cell sizes and compared with previously acquired data [10].

Methods

A shadowgraph apparatus was utilized to record the diffusion process of the iron oxide Fe_2O_3 nanocolloid suspension, sized between 1 to 10 nm. As seen in Fig. 1, an optical bench positioned vertically on a vibration-free table has the glass cell centered along the optical axis. Two achromatic lenses are placed on the top and bottom of the cell distanced at the focal length of the lenses to uniformly illuminate the cell. A CCD camera is placed at the top of the optical bench to record the free diffusion process below. Finally, an SLD is placed at the bottom of the structure at the focal point of the bottom achromatic lens.

The free diffusion process begins when a Fe_2O_3 solution is injected into a glass cell filled with pure water. A free diffusion process in general is linear in its concentration difference. Concentration fluctuations appear as small pockets of fluid that interact with the water and eventually diffuse. The effect of gravity on the concentration gradient, or the particles' procession from higher to lower densities, can be analyzed through the plot of the characteristic time of this free diffusion process.

Once the entire diffusion process is recorded, a differential dynamic algorithm (DDA) extracts the structure function describing the dynamics of the fluctuations. This algorithm takes the following steps:

Frame Extraction: In this stage, the algorithm divides the recording into individual frames. These are gray level images in which the intensity of the pixels corresponds to gray level, where a darker gray indicates the pixel intensity is higher.

Normalization: This step decreases the effects of variability of the light source. The normalization process, defined as

$$i(\boldsymbol{x},t) = I(\boldsymbol{x},t)/I_{avg}\,(\boldsymbol{x},t),$$

is the process by which every pixel value in the image, $I(\boldsymbol{x},t)$ is reassigned to a new value. This new $i(\boldsymbol{x},t)$, value, is the previous pixel value divided by the average pixel value, $I_{avg}\,(\boldsymbol{x},t)$, of the entire image.

Fluctuation Images: These images are the resultant image after the subtraction of two normalized frames separated by a specific time delay, Δt. For delay times much shorter than 100 seconds the frames are too similar, and the signal is subsequently subtracted out. However, for delay times much longer than that, the frames are not correlated at all and the fluctuation image consists of only noise [10]. Fluctuation images are found by

$$\partial i(\boldsymbol{x},t,\Delta t) = i(\boldsymbol{x},t+\Delta t) - i(\boldsymbol{x},t).$$

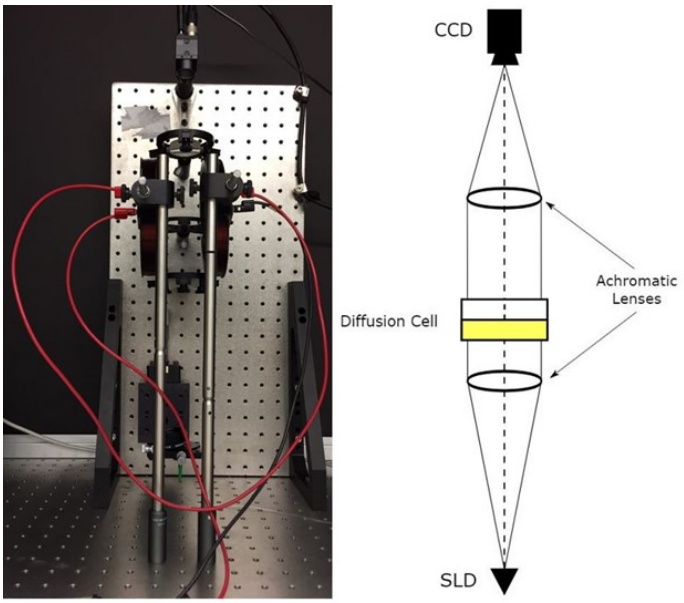

Figure 1: The shadowgraph apparatus in the actual experimental setup (left) and in schematics (right) including a super luminous diode, achromatic lenses, a replaceable diffusion cell, and a CCD camera.

2-D Fourier Transform: The Fourier Transform converts the image from the spatial domain into Fourier space, or the frequency domain, for analysis. In MATLAB, this is represented as

$$\partial i(\boldsymbol{q}, t, \Delta t) = FFT2[\partial i(\boldsymbol{x}, t, \Delta t)]$$

where **q** is a new variable called the wavenumber, defined as 2π/λ, where λ is the wavelength of a fluctuation equaling $n\Delta x$. This Δx refers to the pixel resolution, or the width of the pixel. For our Sony XCL-X700 CL CCD camera, Δx = 4.65 microns.

2-D Power Spectrum: We define the power spectrum as the absolute value of the squared Fourier transform, where

$$|\partial i(\boldsymbol{q}, t, \Delta t)|^2$$

which averages outwards from the center, obtaining power as a function of wavenumber, q.

Radial Average Power Spectrum: The power spectrum is symmetric, similarly to a two-dimensional Gauss-like shape. As a result, we slice it through its center and average all slices. This radial average power spectrum is given by

$$c_m(\boldsymbol{q}, t, \Delta t) = Avg(|\partial i(\boldsymbol{q}, t, \Delta t)|^2)$$

Where c_m gives the power as a function of wavenumber, q, at a constant delay time, Δt .

Structure Function: The algorithm then transposes the radial average power spectrum matrix it just created to obtain the structure function. This new function, given by

$$C_m(\boldsymbol{q}, t, \Delta t) = Avg(c_m(\boldsymbol{q}, t, \Delta t))_q,$$

provides information about the temporal evolution of the power for every wavenumber, q. Thus a plot of the structure function describes how average of the power changes with time, at constant wavenumbers. The structure function is related to the correlation function of fluctuations [11, 12]. In general,

$$C_m(q, t, \Delta t) = 2\big[S(q,t)T(q)\big(1 - G(q, t, \Delta t)\big) + B(q, t)\big],$$

where $G(q, t, \Delta t)$ is the correlation function of the fluctuations and $S(q, t)$ is the structure factor, which describes the amplitude of the fluctuations over time. In some cases, the structure function can be fitted to

$$C_m(q, t, \Delta t) = 2\left[S(q,t)T(q)\left(1 - e^{-\Delta t/\tau(q,t)}\right) + B(q, t)\right],$$

if the correlation function, $G(q, t, \Delta t)$, can be accurately captured by a single decaying exponential. From this fitting we extracted the structure factor, $S(q,t)T(q)$, which provides information about how large the concentration fluctuations are, and the correlation time, $\tau(q, t)$, which provides information about the lifetime of the fluctuations. In general the correlation time of the fluctuations could be related to diffusion and viscosity processes [11, 12]. Through a further fitting process to

$$\tau(q, t) = \frac{1}{Dq^2(1+(\frac{q_c}{q})^4)},$$

we can extract the diffusion coefficient, D. In this relation, q_c refers to the critical wavenumber, which marks the boundary between the diffusive and gravitational regimes. For wavenumbers below this critical value, the correlation time is proportional to q^2 since the force of gravity becomes dominant over that of diffusion on these larger fluctuations. In the case of wavenumbers much higher than the critical value, the correlation time becomes proportional to $\frac{1}{Dq^2}$ and the forces of diffusion dominate the dynamics of these smaller fluctuations.

This entire process was repeated for cylindrical cells with heights of 0.2 cm, 0.5 cm, 1.0 cm, and 2.0 cm all with a constant 2.0 cm diameter. After attaching a pair of Tetron Helmholtz Coils (3B Scientific, 320 turns with 138 mm coil diameter) to the optical bench, a horizontal magnetic field was applied to the 1.0 cm cell and the data gathering process repeated. A constant dc current through the Helmoltz coils was maintained by an Instek PSP-405 Programmable Switching DC Power Supply.

The physical characteristics of each system and cell type was subsequently compared and analyzed to investigate the effect of confinement on the characteristic times and the diffusive coefficients. The film of the free diffusion process was recorded at one frame per second. For the thick cell with a height of 2.0 cm we recorded for 2 days and for the thin cell with a height of 0.2 cm we only recorded for 6 hours. The recording time was estimated by the theoretically determined diffusion time [11, 12].

Results

The cells were prepared with a strong concentration gradient and the diffusion process was recorded for a variable time determined by the anticipated diffusion time. The fluctuation images created from this recording are used to determine the power spectrum for different fixed delay times. A Fourier transform is applied to these fluctuation images to determine their corresponding wavenumber-space images. In wavenumber-space the power spectrum has azimuthal symmetry and can be averaged radially. As shown in Fig. 2, the radial average power spectra transitions from a very small slope to a significantly larger slope at the critical wavenumber. Larger delay times, Δt , result in higher amplitudes in the radial average power spectra. The fluctuation images created using large delay times naturally has more information and thereby more power. The flat horizontal power spectrum at large wavenumbers is determined by the limited resolution of the CCD camera.

The structure functions shown in Fig. 3 represent a cross section of the corresponding radial average power spectra at fixed wavenumbers. They tell us about the temporal evolution of the power spectra, with a positive slope as a result of the power spectrum's positive relation with delay time explained previously. Since the wavenumber is inversely proportional to the size of the fluctuations, the smaller wavenumbers have larger amplitudes in the structure function.

The structure function, $C_m(q, t, \Delta t)$, was fitted using Eqn. 7. From this process the structure factor, $S(q,t)T$ was extracted. This factor is a product of the real structure factor, $S(q,t)$, and the shadowgraph transfer function, $T(q)$. In our trials, the background fluctuation noise, $B(q,t)$, was at least one order of magnitude smaller than the experimental structure factor, giving us a full range of viable wavenumbers.

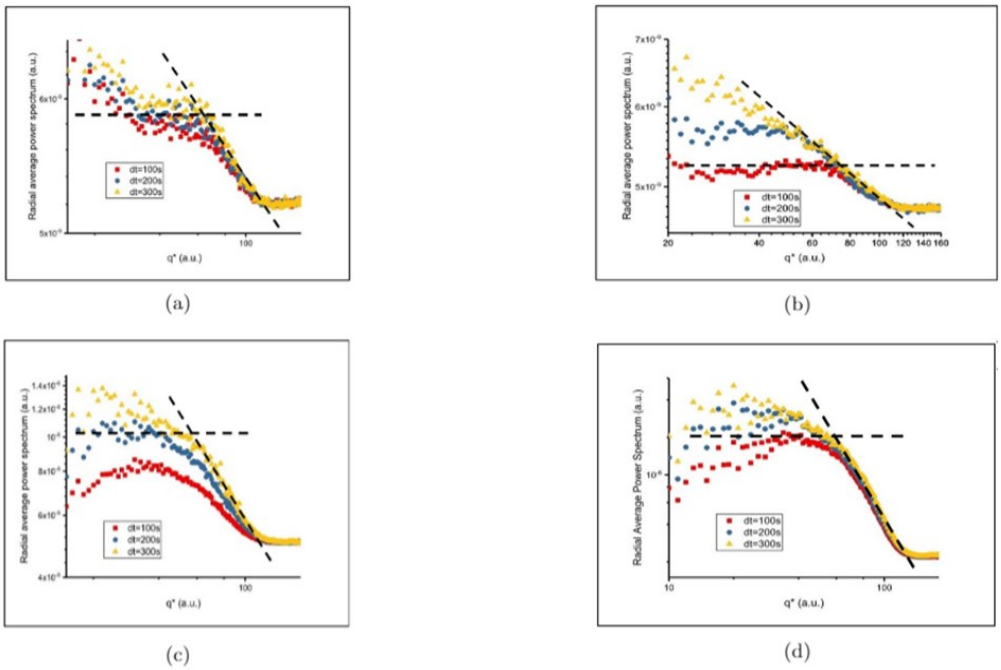

Figure 2: Radial average power spectra of free diffusion in a) 0.2 cm b) 0.5 cm c) 1.0 cm d) 2.0 cm cells. The transition from almost no slope to a large slope power spectrum takes place around the critical wavenumber.

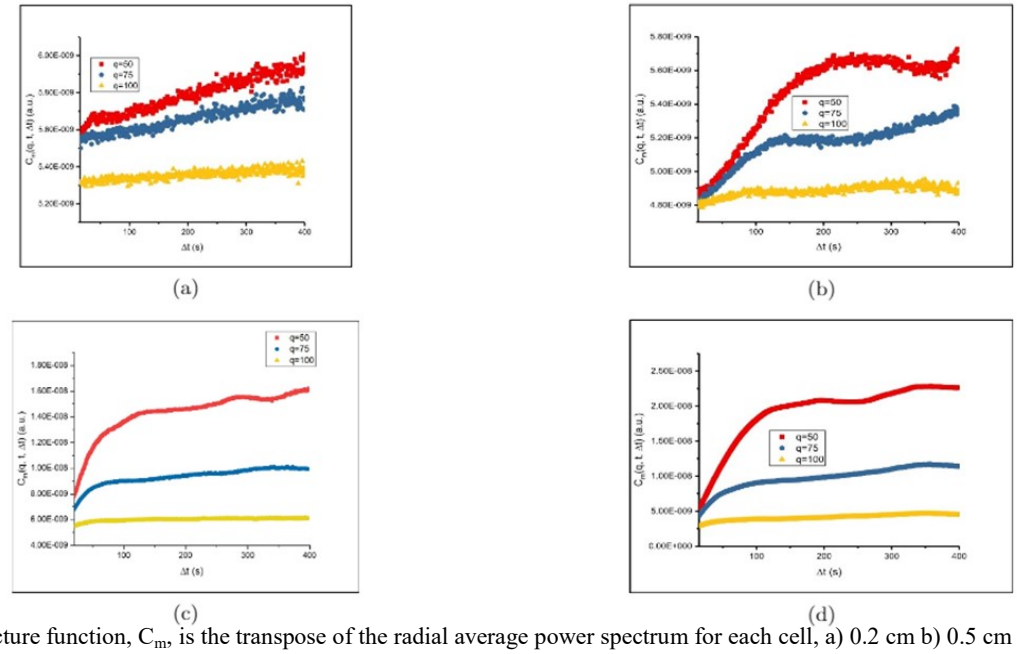

Figure 3: The structure function, C_m, is the transpose of the radial average power spectrum for each cell, a) 0.2 cm b) 0.5 cm c) 1.0 cm d) 2.0 cm.

Figure 4: a) Comparison of structure factors in free diffusion for the different cell geometries. The amplitude decreases along with cell height. b) The structure factor of the 1.0 cm cell with an applied horizontal magnetic field. The slope transition in the power spectrum determines the critical wavenumber, q_c.

As shown in Fig. 4, the structure factor seems almost entirely horizontal in the region below the critical wavenumber. This unchanging region is a result of the buoyancy effects of the gravitational force. In the region above the critical wavenumber, a steep characteristic slope proportional to q^{-4} can be observed. Also importantly observed in Fig. 4(a) is the dampening of the amplitude of the structure factor as cell height decreases. The effect of the horizontal magnetic field is seen in Fig. 4(b) through a shift of the critical wavenumber.

Similarly to the structure factor, we used Eqn. 9 to extract the correlation time, which tells us about the lifetime of the fluctuations. The characteristic gravity and diffusion regimes of the process are easily seen through the plots of the correlation time in Fig. 5. When the slope of the correlation time transitions to a negative value at the critical wavenumber, the diffusion regime begins and signifies a range of wavenumbers that live long enough for diffusion to occur. A shift in the critical wavenumber downwards as cell height decreases indicates that the diffusive mode follows a q^{-2} power law, as follows from Eqn. 9 regarding the correlation time of large scale fluctuations.

In the presence of a magnetic field, the slope of the structure factor decreased to a lower power law. We found this magnetic field caused the rate of diffusion to decrease. When the horizontal magnetic field is applied, the nanoparticles align themselves with it in rod-like structures. These rods could scatter incident light back and decrease the overall intensity of detected light, although more research is needed to fully examine the effect of the horizontal magnetic field.

Conclusions

The unique changes in the dynamics of concentration gradient driven fluctuations based on cell size were analyzed using a direct imaging method. The confinement of the diffusion process of iron oxide nanoparticles led to changes in such analytically studied properties as the radial average power spectrum, the structure function, the structure factor, and the correlation time. Secondarily, the effect of an applied horizontal magnetic field was investigated shortly, and those same diffusion properties were determined.

We concluded that the confinement of the free diffusion space leads to a dampening of amplitude of the structure factor while still maintaining a characteristic q^{-4} power law. In investigating the correlation time, we found that gravitational mode naturally follows a q^2 power law, and that

Notes and References

*Corresponding author email: OprisanA@cofc.edu

[1] A. Vailati, M. Giglio, Nature 390, 262 (1997).
[2] J.M. Ortiz de Z´arate, J.V. Sengers, Physica A 300, 25 (2001).
[3] T. Kirkpatrick, J. Ortiz de Zarate, J. Sengers, Phys. Rev. Lett. 115, 035901 (2015).
[4] T.R. Kirkpatrick, J.M. Ortiz de Z´arate, J.V. Sengers, Phys. Rev. E 93, 012148 (2016).
[5] T.R. Kirkpatrick, J.M. Ortiz de Z´arate, J.V. Sengers, Phys. Rev. E 93, 032117 (2016).
[6] S.P. Trainoff, D.S. Cannell, Phys. Fluids 14, 1340 (2002).
[7] M.E. Fisher, P.G. de Gennes, C. R. Acad. Sci. Ser. B 287, 207 (1978).
[8] H.B.G. Casimir, Proc. K. Ned. Akad. Wet. 51, 793 (1948).
[9] R.A. Frimpong, J.Z. Hilt, Nanomedicine 5, 1401 (2010).
[10] Oprisan, A., Rice, A., Oprisan, S.A. et al. Eur. Phys. J. E (2017) 40: 14.
[11] F. Croccolo, D. Brogioli, Appl. Opt. 50, 3419 (2011).
[12] F. Croccolo, D. Brogioli, A. Vailati, M. Giglio, D.S. Cannell, Phys. Rev. E 76, 041112 (2007).

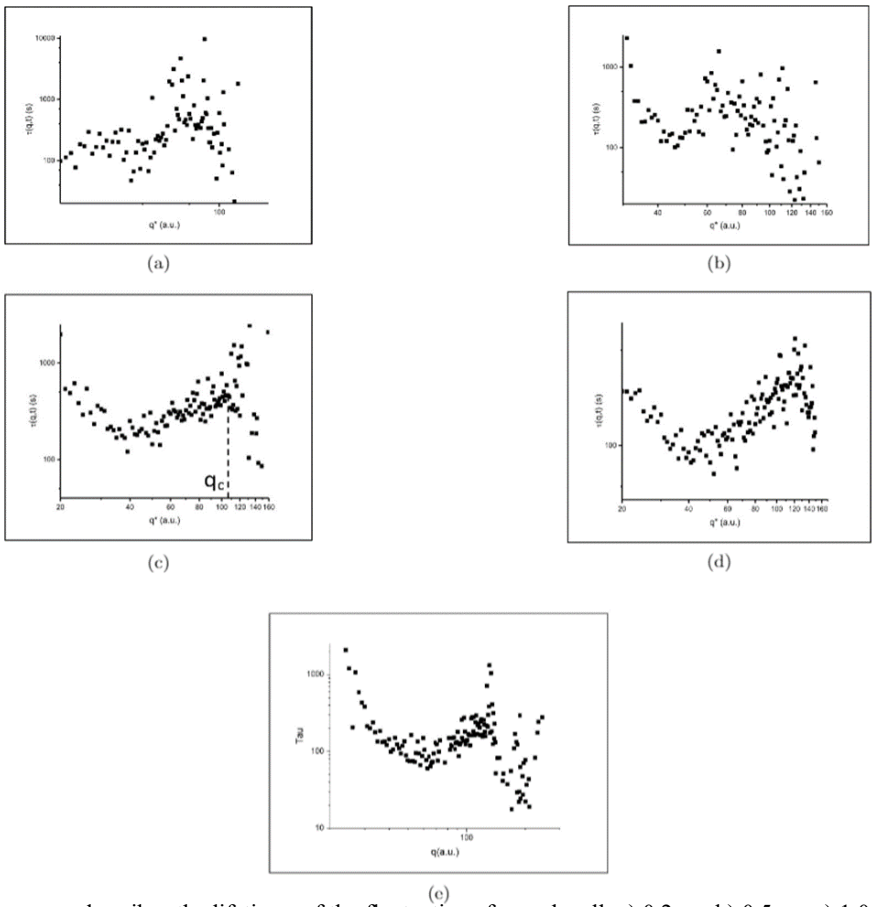

Figure 5: The correlation time, τ , describes the lifetimes of the fluctuations for each cell, a) 0.2 cm b) 0.5 cm c) 1.0 cm d) 2.0 cm, as a function of wavenumber. The correlation time for e) the 1.0cm cell with an applied horizontal magnetic field observed a shifting of the critical wavenumber to a higher value.